HOKKAIDO UNIVERSITY

Title	Three-Dimensional Wake Field Computations Based on Scattered-Field Time Domain Boundary Element Method
Author(s)	Fujita, Kazuhiro; Kawaguchi, Hideki; Weiland, Thomas et al.
Citation	IEEE Transactions on Nuclear Science, 56(4-3), 2341-2350 https://doi.org/10.1109/TNS.2009.2025042
Issue Date	2009-08
Doc URL	https://hdl.handle.net/2115/39220
Rights	© 2009 IEEE. Personal use of this material is permitted. However, permission to reprint/republish this material for advertising or promotional purposes or for creating new collective works for resale or redistribution to servers or lists, or to reuse any copyrighted component of this work in other works must be obtained from the IEEE.
Type	journal article
File Information	TNS56-4-3_p2341-2350.pdf

Hokkaido University Collection of Scholarly and Academic Papers : HUSCAP

Three-Dimensional Wake Field Computations Based on Scattered-Field Time Domain Boundary Element Method

Kazuhiro Fujita, Hideki Kawaguchi, Thomas Weiland, and Satoshi Tomioka

***Abstract*—We present time domain 3-D wake field calculations based on Scattered-field Time Domain Boundary Element Method (S-TDBEM), which is retarded Kirchhoff's boundary integral equations of scattered electromagnetic fields formulated on interior region problem and has no numerical dispersion in all spatial direction. We propose two main types of S-TDBEM schemes: full 3-D scheme for general 3-D geometries and a so-called 2.5-D scheme for transverse wake field calculation in axis-symmetric structures. Several numerical examples are demonstrated for typical accelerator structures: elliptical pillbox and the TESLA 9-cell cavities. The developed 3-D/2.5-D S-TDBEM codes are verified by comparison with the modal analysis and the finite integration technique (FIT) in the numerical examples. Finally, as one of the most meaningful applications of the S-TDBEM, we demonstrate wake field simulations of a curved trajectory bunch with the developed 3-D S-TDBEM code.**

***Index Terms*—Boundary element method, dispersion-free, synchrotron radiation, wake fields, wake potential.**

I. Introduction

INCREASED demands for very short and high-intensity electron bunches in advanced accelerator projects such as linear colliders and X-ray free electron lasers motivate accurate understanding of short-range wake fields [1] and precise prediction of beam dynamics effects such as emittance growth and energy spread. Many sophisticated computer codes based on Finite Integration Technique (FIT) [2] and Finite Element Method (FEM) [3] have been developed, and successfully applied for many practical cases. However, in recent accelerator applications the following problems are recognized to be difficult even with such FIT-based approaches: short-range wake field simulations of a short bunch in long accelerator structures and transient analysis of wake fields excited by a bunch moving with curved trajectories in arbitrarily shaped 3-D vacuum chambers. For the former, several dispersionless algorithms have been proposed in the context of FIT [4]–[7]. In the latter, however, the applicability of the existing FIT/FEM codes may be still severely limited by the numerical dispersion errors of finite difference scheme used in their codes.

In order to handle the above two problems, we have been working on the development of wake field analysis based on Time Domain Boundary Element Method (TDBEM) [8]–[12], which discretizes the charges and the currents on the boundary surface and solves retarded Kichhoff's boundary integral equations directly in time domain. The TDBEM has several advantages in wake field analysis: zero dispersion in all spatial direction, conformal modeling of arbitrary 3-D geometries and treatment of a bunch of charged particles with curved trajectories.

So far, a TDBEM formulation based on time domain Kirchhoff's boundary integral equations for the total electromagnetic fields was discussed, and the stable time domain simulation scheme was presented [8]–[10]. For 3-D problems, however, the simulations can be performed only for modest numerical models [10] because applicable model size is severely limited by very large memory requirements of the 3-D TDBEM scheme. In order to deal with practical long accelerator structures in the framework of TDBEM, the integral equation formulation of moving window technique was proposed [11]. This moving window technique was combined with a TDBEM scheme based on the scattered field formulation [12] which is called as Scattered-field Time Domain Boundary Element Method (S-TDBEM). The 2-D S-TDBEM calculations with moving window technique were applied for the TESLA accelerator cavities and tapered collimators [11].

The aim of this paper is to present practical 3-D wake field simulations by the S-TDBEM. In the framework of S-TDBEM, a full 3-D scheme is firstly proposed, and followed by an axisymmetric 3-D scheme with reduced memory requirements. We newly introduce a quasi 3-D algorithm based on the azimuthal Fourier series expansion, which is often called as 2.5-D scheme, for fast calculation of transverse wake fields of an offset bunch traversing in axisymmetric accelerator structures. Some numerical examples for typical accelerating cavities are presented in order to validate the developed full 3-D and 2.5-D codes.

Finally we demonstrate 3-D simulations of wake fields excited by a curved trajectory bunch with the developed code.

II. Time Domain Integral Equation for Scattered Electromagnetic Fields

We are interested in a coupled problem of a charged particle beam and an accelerator structure with perfectly conducting walls. We assume here that the beam is moving in a domain

Manuscript received December 17, 2008; revised April 30, 2009. Current version published August 12, 2009. This work was supported in part by a research grant from the Hokkaido University Clark Memorial Foundation.

K. Fujita and S. Tomioka are with the Division of Quantum Science and Engineering, Graduate School of Engineering, Hokkaido University, Kita-ku, Sapporo 060-8628, Japan (e-mail: fujita@athena.qe.eng.hokudai.ac.jp).

H. Kawaguchi is with the Department of Electrical and Electronic Engineering, Muroran Institute of Technology, Muroran 050-8585, Japan.

T. Weiland is with the Institute fuer Theorie Electromagnetischer Felder, Technishe Universitaet Darmstadt, D-64289 Darmstadt, Germany.

Digital Object Identifier 10.1109/TNS.2009.2025042

0018-9499/$26.00 © 2009 IEEE

Authorized licensed use limited to: HOKKAIDO DAIGAKU KOHGAKUBU. Downloaded on September 7, 2009 at 03:22 from IEEE Xplore. Restrictions apply.

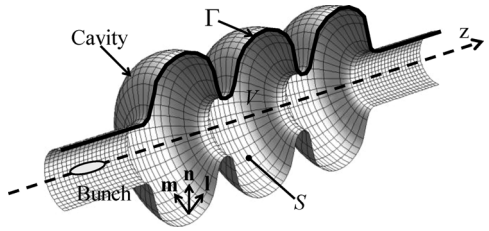

Fig. 1. Typical example of wake field analysis: a charged particle bunch traversing an axially symmetric accelerating cavity.

V which is bounded transversely by the boundary surface S of accelerator structures with ingoing and outgoing pipes such as accelerating cavities (see Fig. 1). The particle bunch with a fixed but arbitrarily shape along a given bunch trajectory is assumed through this paper, and therefore the beam-surroundings system is not solved self-consistently. Then, our interest is to obtain wake fields in the domain for a given bunch distribution in the framework of time domain boundary integral equation formulation.

In general, the electromagnetic fields $(\mathbf{E}, \mathbf{B})$ inside an accelerator structure can be expressed as a superposition of the bunch self-fields $(\mathbf{E}_{self}, \mathbf{B}_{self})$ in free space and the scattered fields $(\mathbf{E}_{scat}, \mathbf{B}_{scat})$:

$$\mathbf{E} = \mathbf{E}_{self} + \mathbf{E}_{scat},\ \mathbf{B} = \mathbf{B}_{self} + \mathbf{B}_{scat}. \tag{1}$$

The bunch self-fields in the pipe can be given analytically or obtained numerically. For example, the self-field of an on-axis bunch moving at the speed of light in an infinitely long pipe with circular cross section of radius a can be described in cylindrical coordinate as follows [1]:

$$E_r(r,\theta,z,t) = \frac{\rho_z(z-ct)}{2\pi\varepsilon_0 r},\ B_\varphi(r,\theta,z,t) = \frac{E_r}{c},\ r \le a \tag{2}$$

where the line charge distribution ρ is given by

$$\rho(r,\theta,z,t) = \delta(r)\,\rho_z(z-ct), \tag{3}$$

where $\delta(r)$ is the Dirac's delta function. For a bunch with arbitrarily curved trajectory, the self-field $(\mathbf{E}_{self}, \mathbf{B}_{self})$ in free space can be obtained by numerical integrations of charge distribution $\rho(\mathbf{r},t)$, $\mathbf{J}(\mathbf{r},t)$ from the retarded potential formula [13]:

$$\mathbf{E}_{self}(\mathbf{r},t) = -\frac{\partial \mathbf{A}}{\partial t} - \nabla\phi,\ \mathbf{B}_{self}(\mathbf{r},t) = \nabla\times\mathbf{A} \tag{4}$$

$$\phi(\mathbf{r},t) = \frac{1}{4\pi\varepsilon_0}\int_v \frac{\rho(\mathbf{r}',t')}{|\mathbf{r}-\mathbf{r}'|}dV',$$

$$\mathbf{A}(\mathbf{r},t) = \frac{\mu_0}{4\pi}\int_v \frac{\mathbf{J}(\mathbf{r}',t')}{|\mathbf{r}-\mathbf{r}'|}dV' \tag{5}$$

with the retarded time $t' = t - |\mathbf{r}-\mathbf{r}'|/c$.

The scattered fields $\mathbf{E}_{scat}$ and $\mathbf{H}_{scat}$ can be described by the following time domain Kirchhoff's integral equation of scattered electric and magnetic field on interior problems with homogeneous material constants ε_0, μ_0 [12]: [see equations (6) and (7) at the bottom of the page] where $\mathbf{r}$ is the observation point in the interior region, $\mathbf{r}'$ is the position vector on the surface, $R = |\mathbf{r}-\mathbf{r}'|$, $c^2 = 1/\varepsilon_0\mu_0$, t' is the retarded time, and $\mathbf{n}'$ is the inward unit vector normal to the surface. The fields on the boundary S are related to the equivalent surface electric and magnetic current densities $(\mathbf{K}_\mathrm{s}, \mathbf{M}_\mathrm{s})$ and charge densities $(\sigma_\mathrm{s}, \eta_\mathrm{s})$ by

$$\begin{aligned}
\mathbf{n}\times\mathbf{E}_{scat} &= -\mathbf{n}\times\mathbf{E}_{self} = -\mathbf{M}_\mathrm{s}\\
\mathbf{n}\times\mathbf{B}_{scat} &= -\mathbf{n}\times\mathbf{B}_{self} + \mu_0\mathbf{K} = \mu_0\mathbf{K}_\mathrm{s}\\
\mathbf{n}\cdot\mathbf{E}_{scat} &= -\mathbf{n}\cdot\mathbf{E}_{self} + \frac{\sigma}{\varepsilon_0} = \frac{\sigma_\mathrm{s}}{\varepsilon_0}\\
\mathbf{n}\cdot\mathbf{B}_{scat} &= -\mathbf{n}\cdot\mathbf{B}_{self} = \eta_\mathrm{s}
\end{aligned} \tag{8}$$

with the real surface charge density σ and current density $\mathbf{K}$ due to the total fields. Since the equivalent surface sources $\mathbf{K}_\mathrm{s}$, $\mathbf{M}_\mathrm{s}$, σ_s, and η_s are related to the boundary condition of perfect conductor, the bunch self-fields indirectly excite the wake fields though $\mathbf{M}_\mathrm{s}$ and η_s in (8).

A set of the integral (6) and (7) is a time domain description of Kirchhoff boundary integral equation of the scattered fields, and it can be physically interpreted as a Huygens principle of scattered electromagnetic fields.

$$\begin{aligned}
\mathbf{E}_{scat}(\mathbf{r},t) = -\frac{1}{4\pi}\oint_S \Bigg\{ &(\mathbf{n}'\times\mathbf{E}_{scat}(\mathbf{r}',t'))\times\nabla'\frac{1}{R} - \frac{1}{R}\left(\mathbf{n}'\times\frac{\partial\mathbf{E}_{scat}}{c\partial t}(\mathbf{r}',t')\right)\times\nabla' R\\
&+ (\mathbf{n}'\cdot\mathbf{E}_{scat}(\mathbf{r}',t'))\nabla'\frac{1}{R} - \frac{1}{R}\left(\mathbf{n}'\cdot\frac{\partial\mathbf{E}_{scat}}{c\partial t}(\mathbf{r}',t')\right)\nabla' R - \frac{1}{R}\left(\mathbf{n}'\times\frac{\partial\mathbf{B}_{scat}}{\partial t}(\mathbf{r}',t')\right)\Bigg\}dS',
\end{aligned} \tag{6}$$

$$\begin{aligned}
\mathbf{B}_{scat}(\mathbf{r},t) = -\frac{1}{4\pi}\oint_S \Bigg\{ &(\mathbf{n}'\times\mathbf{B}_{scat}(\mathbf{r}',t'))\times\nabla'\frac{1}{R} - \frac{1}{R}\left(\mathbf{n}'\times\frac{\partial\mathbf{B}_{scat}}{c\partial t}(\mathbf{r}',t')\right)\times\nabla' R\\
&+ (\mathbf{n}'\cdot\mathbf{B}_{scat}(\mathbf{r}',t'))\nabla'\frac{1}{R} - \frac{1}{R}\left(\mathbf{n}'\cdot\frac{\partial\mathbf{B}_{scat}}{c\partial t}(\mathbf{r}',t')\right)\nabla' R + \frac{1}{R}\left(\mathbf{n}'\times c^{-2}\frac{\partial\mathbf{E}_{scat}}{\partial t}(\mathbf{r}',t')\right)\Bigg\}dS',
\end{aligned} \tag{7}$$

Authorized licensed use limited to: HOKKAIDO DAIGAKU KOHGAKUBU. Downloaded on September 7, 2009 at 03:22 from IEEE Xplore. Restrictions apply.

III. Numerical Formulation

In this work, we adapt the magnetic (scattered) field integral equation (MFIE) in time domain (7) as a fundamental equation. The two tangential components and the normal component of the magnetic field are appeared in the MFIE (7). Unlike the axisymmetric 2-D S-TDBEM scheme [12], the normal component of the magnetic fields does not vanish in full 3-D schemes, but it is not unknown boundary value because of the boundary conditions (8). Therefore, we have only two tangential components of magnetic field on the boundary as unknown boundary values.

A. Discretization of Integral Equation

The surface S is discretized with spatial quadrilateral planar patches as boundary element and the time axis is divided by constant time step size Δt. The fields ($\mathbf{n}\times\mathbf{B}_{scat}\equiv\mathbf{B}_t$, $\mathbf{n}\cdot\mathbf{B}_{scat}\equiv B_n$ and $\mathbf{n}\times\mathbf{E}_{scat}\equiv\mathbf{E}_t$) on a boundary element are spatially expanded into the 2-D curl-conforming basis functions [14] $\mathbf{f}_i(\mathbf{r})$ for vectorial quantities, the zero-order basis function $g_i(\mathbf{r})$ for scalar quantity, and temporally expanded into the local triangular basis function $T_k(t)$ (i.e., linearly-interpolated temporally):

$$\mathbf{B}_t(\mathbf{r},t)=\sum_{k=0}^{\infty}\sum_{i=1}^{2N_e} {b_t}^{i,k}\mathbf{f}_i(\mathbf{r})T_k(t), \tag{9}$$

$$B_n(\mathbf{r},t)=\sum_{k=0}^{\infty}\sum_{i=1}^{N_e} {b_n}^{i,k} g_i(\mathbf{r})T_k(t), \tag{10}$$

$$\mathbf{E}_t(\mathbf{r},t)=\sum_{k=0}^{\infty}\sum_{i=1}^{2N_e} {e_t}^{i,k}\mathbf{f}_i(\mathbf{r})T_k(t), \tag{11}$$

where N_e is the number of patches on the surface. The time derivative is approximated by backward finite difference. The boundary integrations can be numerically performed by taking into account the retarded time on the discretized time axis.

After performing this discretization procedure, we finally have the following matrix equation:

$$[G_0]\,{\mathbf{b}_t}^n=\sum_{k=1}^{n}[G_k]\,{\mathbf{b}_t}^{n-k}+\sum_{k=0}^{n}[C_k]\,{\mathbf{b}_n}^{n-k}+\sum_{k=0}^{n}[P_k]\,{\mathbf{e}_t}^{n-k}, \tag{12}$$

where $\mathbf{b}_t^i$, $\mathbf{b}_n^i$ and $\mathbf{e}_t^i$ denote the boundary value vectors which consist of the tangential and normal magnetic field components and the tangential electric field component on the boundary elements at time $t=i\Delta t$ ($i=0,\ldots,K$), respectively. $[G_k]$, $[C_k]$ and $[P_k]$ denote coefficient matrices determined by the boundary integral of (7), respectively. Then, the vectors $\mathbf{b}_n^i$ and $\mathbf{e}_t^i$ are always known because they can be calculated directly from the bunch self-fields by (8). Therefore we finally obtain a system matrix equation as follows:

$$[G_0]\;{\mathbf{b}_t}^n={\mathbf{b}_{ext}}^n+\sum_{k=1}^{n}[G_k]\;{\mathbf{b}_t}^{n-k}, \tag{13}$$

where the vector $\mathbf{b}_{ext}^n$ is the resulting vector from the second and third terms of (12) at a time step n. By solving the reduced matrix (13) at each time step, the electric surface current and charge densities induced on the boundary surface of an accelerator structure can be obtained iteratively. The second and third terms of $\mathbf{b}_n^i$ and $\mathbf{e}_t^i$ over all time steps should be in advance calculated before the system matrix (13) is solved.

Once the boundary values have been obtained over all time steps, the wake fields at any position in the bounded domain can be calculated from (6) and (7).

The time domain scheme (13) can be categorized by the relation between $c\Delta t$ and the minimum facet size $h_{\min}$ or the maximum facet size $h_{\max}$. The matrix $[G_0]$ is diagonal for $c\Delta t < h_{\min}$, and therefore inversion of the matrix is very easy. This is usually called explicit scheme. On the other hand, the matrix $[M_0]$ is non-diagonal for $c\Delta t > h_{\max}$, and then the sparse matrix $[G_0]$ can be solved by conventional iterative matrix solutions such as the Conjugate Gradient Squared (CGS) method. This scheme is called implicit scheme.

B. Full 3-D and Axisymmetric 3-D Schemes

The S-TDBEM proposed above has applicability to wake field simulations of arbitrary 3-D geometries, but its straightforward implementation is computationally expensive. The required memory of S-TDBEM scheme for 3-D problems can be estimated as follows: if the number of the patches on a surface is of order of $N_e = N^2$, where N is the number of division in one-dimension, then the number of elements in each of the boundary value vectors $\mathbf{b}_t^i$ and $\mathbf{e}_t^i$ becomes $2N^2$ (N^2 for $\mathbf{b}_n^i$) and the number of the matrices K is same order as N. Therefore, the required memory size can be estimated as $8\times 2N^2\times 2N^2\times K$ Byte in double precision floating point calculation. For example, the required memory size reaches about 10 T Byte for $N^2 = 40000$, $K = 200$. However, taking into account the sparseness of the matrices $[G_k]$, one can compress the required memory size into the order of $8\times 2N^2\times\alpha\times N\times K$ Byte, where α is an compression factor depending on the sparseness of the matrices. Then, the memory size of the 3-D S-TDBEM scheme becomes about 380 G Byte for the same example $N^2 = 40000$, $\alpha = 15$, $K = 200$.

If the geometry of a numerical model is assumed to be axisymmetric as sometimes appeared in practical accelerator structures, then all of the matrices $[G_k]$, $[C_k]$ and $[P_k]$ in the original matrix (12) have a cyclic symmetry and effective memory size reduction for the system matrices is possible even for 3-D field problems [8]–[10], because matrix elements can be calculated only from the distance $|\mathbf{r}-\mathbf{r}'|$ and the inner products between the vector $(\mathbf{r}-\mathbf{r}')$ and local basis functions depending on patch geometries. Using the sparseness and this cyclic symmetry of the matrices, we can reduce the required memory for the above 3-D S-TDBEM scheme into the order of $8\times 2N^2\times\alpha\times K$. In fact, the total memory size of this scheme is reduced to about 1.9 G Byte for $N^2 = 40000$, $\alpha = 15$, $K = 200$. We shall call this as axisymmetric 3-D S-TDBEM scheme (A3D S-TDBEM).

Authorized licensed use limited to: HOKKAIDO DAIGAKU KOHGAKUBU. Downloaded on September 7, 2009 at 03:22 from IEEE Xplore. Restrictions apply.

C. Quasi 3-D Scheme Based on Azimuthal Fourier Series Expansions: 2.5D Algorithm

The A3D S-TDBEM scheme was introduced in order to reduce the memory needs for simulating 3-D wake fields of axially symmetric geometries as in Fig. 1. However, the calculation time of this scheme is almost same as that of the full 3-D S-TDBEM scheme since all of boundary values over the 2-D surface have to be solved at each time step. Note that the bunch shape and its trajectory can be chosen to be arbitrary in the A3D S-TDBEM. Here we propose further reduction of calculation costs of (12) with azimuthal Fourier series expansion of electromagnetic fields excited in axially symmetric structures.

In conventional wake field analysis, the beam is usually modeled as a line charge $J_z(r,\varphi,z,t,)$, and can be expressed as a sum of azimuthal moments (e.g., see [1]):

$$J_z(r,\varphi,z,t) = \sum_{p=0}^{\infty} {j_z}^{(p)} = \sum_{p=0}^{\infty} \frac{c\rho(z-ct)\,\delta(r-a)}{\pi a(1+\delta_{p0})}\cos p\varphi \quad (14)$$

with the beam trajectory offset a to the symmetry axis (the z-axis). The azimuthal moments of the bunch are regarded as rings of charge with a radius of a and with the dependencies of $\cos\, p\varphi$. The scattered fields can be then expanded into the Fourier series in term of the azimuthal dependency of the fields induced inside an axially symmetric structure in cylindrical coordinates (r,φ,z):

$$(e_r, b_\varphi, e_z) = \sum_{p=0}^{\infty} (e_r, b_\varphi, e_z)^{(p)} \cos p\varphi$$
$$(b_r, e_\varphi, b_z) = \sum_{p=0}^{\infty} (b_r, e_\varphi, b_z)^{(p)} \sin p\varphi \quad (15)$$

where

$$\mathbf{E}_{scat} = (e_r, e_\varphi, e_z)$$
$$\mathbf{B}_{scat} = (b_r, b_\varphi, b_z). \quad (16)$$

Note that $\mathbf{E}_{scat}$ and $\mathbf{B}_{scat}$ are dependent of r,φ,z,t, while the coefficients $e_r^{(p)}$, $e_\varphi^{(p)}$, $e_z^{(p)}$, $b_r^{(p)}$, $b_\varphi^{(p)}$ and $b_z^{(p)}$ depend on r, z, t. Since the Maxwell equations for the scattered fields hold individually for each azimuthal mode [15], it is possible to solve only a set of the fields for individual mode p : $e_r^{(p)}$, $e_\varphi^{(p)}$, $e_z^{(p)}$, $b_r^{(p)}$, $b_\varphi^{(p)}$ and $b_z^{(p)}$. This means explicitly that a 3-D problem can be reduced to the sum of 2-D problems for each mode p. This concept has been popularly used in wake field calculation based on FIT schemes [15]–[17].

We apply this dimensional reduction technique for the TDBEM. As a typical example, we consider an axially symmetric structure as shown in the Fig. 1 and define a local coordinate system $(\mathbf{l},\mathbf{m},\mathbf{n}=\mathbf{l}\times\mathbf{m})$. Using these notations, we find from (15) that the field components on the boundary also have the following sine/cosine dependencies:

$$(E_l, B_m, E_n) = \sum_{p=0}^{\infty} (e_l, b_m, e_n)^{(p)} \cos p\varphi$$
$$(B_l, E_m, B_n) = \sum_{p=0}^{\infty} (b_l, e_m, b_n)^{(p)} \sin p\varphi \quad (17)$$

where

$$\mathbf{E}_{scat} = (E_l, E_m, E_n)$$
$$\mathbf{B}_{scat} = (B_l, B_m, B_n)$$
$$\text{on boundary.} \quad (18)$$

Again, note that the coefficients $e_l^{(p)}$, $e_m^{(p)}$, $e_n^{(p)}$, $b_l^{(p)}$, $b_m^{(p)}$ and $b_n^{(p)}$ depend on r, z, t. Substitution of the Fourier series expansions (17) into the integral (6) and (7) yields integral equations of the scattered fields for the individual mode p. From (7) and (17), we can easily obtain the following magnetic field integral equations for any azimuthal mode p in cylindrical coordinates (r,φ,z):

$${b_l}^{(p)}(r,z,t) = -\frac{1}{4\pi\sin(p\varphi)}\mathbf{l}\cdot{\mathbf{b}_{az}}^{(p)}(r,z,t)$$
$${b_m}^{(p)}(r,z,t) = -\frac{1}{4\pi\cos(p\varphi)}\mathbf{m}\cdot{\mathbf{b}_{az}}^{(p)}(r,z,t), \quad (19)$$

where [see equation (20) at the bottom of the page] and then the integrands in (20) depend on (r',z',t'). A set of the two integral (19) can be spatially and temporally discretized as in Section III-A. The resulting system matrix equation for the mode p

$$\begin{aligned}{\mathbf{b}_{az}}^{(p)}(r,z,t) = \oint_S \Bigg\{ &\left(\left[{b_l}^{(p)}\right]\sin(p\varphi')\mathbf{m}' - \left[{b_m}^{(p)}\right]\cos(p\varphi')\mathbf{l}'\right)\times\nabla'\frac{1}{R} \\ &-\frac{1}{Rc}\left(\left[\frac{\partial {b_l}^{(p)}}{\partial t}\right]\sin(p\varphi')\mathbf{m}' - \left[\frac{\partial {b_m}^{(p)}}{\partial t}\right]\cos(p\varphi')\mathbf{l}'\right)\times\nabla' R + \left(\left[{b_n}^{(p)}\right]\sin(p\varphi')\right)\nabla'\frac{1}{R} \\ &-\frac{1}{Rc}\left(\left[\frac{\partial {b_n}^{(p)}}{\partial t}\right]\sin(p\varphi')\right)\nabla' R + \frac{1}{Rc^2}\left(\left[\frac{\partial {e_l}^{(p)}}{\partial t}\right]\cos(p\varphi')\mathbf{m}' - \left[\frac{\partial {e_m}^{(p)}}{\partial t}\right]\sin(p\varphi')\mathbf{l}'\right)\Bigg\} dS' \quad (20)\end{aligned}$$

Authorized licensed use limited to: HOKKAIDO DAIGAKU KOHGAKUBU. Downloaded on September 7, 2009 at 03:22 from IEEE Xplore. Restrictions apply.

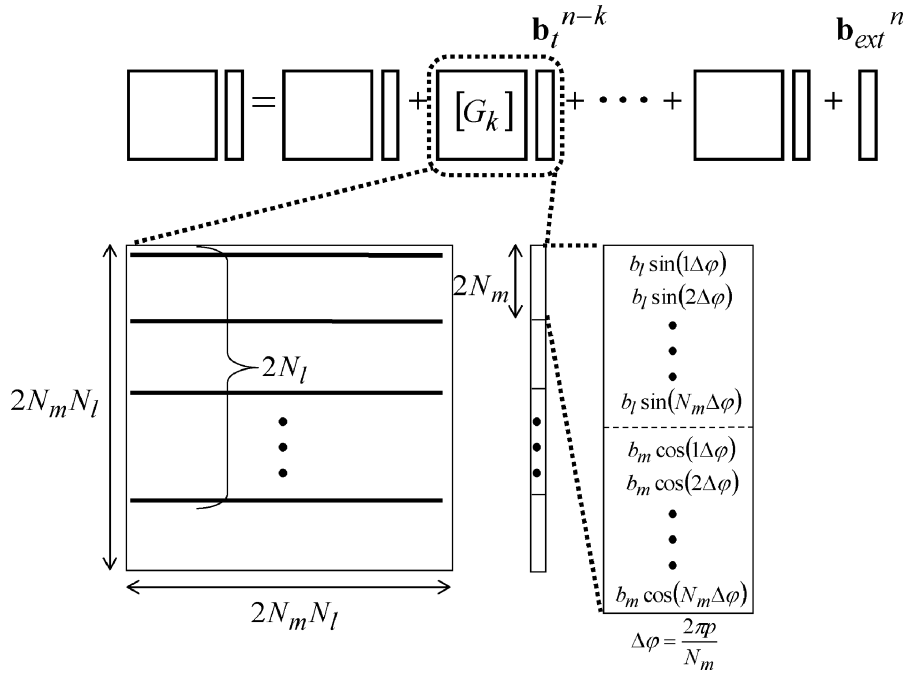

Fig. 2. The $\sin$ / $\cos$ dependencies of boundary value vector in A3D S-TDBEM system matrix equation for azimuthal mode p. In the A3D scheme, one needs to store only first row among the boundary elements with same radius [8]–[10], and therefore matrix size becomes $2N_l \times 2N_lN_m$ without taking into account the sparseness of the matrix. However, in a time domain simulation the amount of overall operation is almost same as that of the full 3-D scheme since all boundary values over a 2-D surface have to be solved.

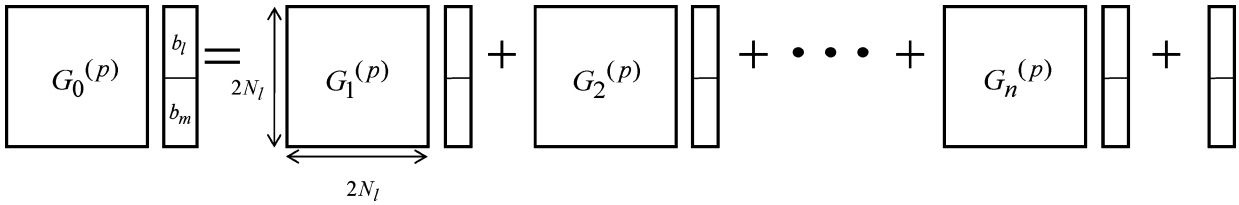

Fig. 3. Structure of the reduced 2.5-D TDBEM matrix equation for azimuthal mode m.

has the same structure as (12), and therefore it can be reduced as in (13) by the same manner. From (19) and (20), we can find that the number of unknown boundary values on the 2-D surface S can be reduced to the 1-D cross-section Γ in Fig. 1. The time domain solution of boundary values for all modes can be calculated by rerunning for each mode.

In order to estimate the numerical costs of this quasi 3-D scheme, we shall consider to apply the A3D S-TDBEM scheme to a 3-D field simulation with the excitation of the ring beam self-fields [1] for a single mode p. Then, the system matrix (13) of the A3D S-TDBEM scheme should have boundary value vectors with sine/cosine dependencies as in Fig. 2. Fig. 3 shows a concrete example of the system matrix equation obtained from (19) for an azimuthal mode p. N_l and N_m are the number of division in the l- and the m-directions, respectively. Therefore, the required memory and the calculation time of this scheme in a single mode calculation become smaller by a factor of $1/N_m$ and $1/N_m^2$ than those of the A3D S-TDBEM scheme, respectively. We shall call this quasi-3D scheme as a 2.5-D S-TDBEM scheme. In this scheme the monopole case ($p = 0$) is corresponding to the axially symmetric field formulation as demonstrated in [12].

The 2.5-D S-TDBEM scheme is especially suitable for transverse wake potential calculations for axially symmetric structures. Due to the radial dependency of the wake potentials [1], the transverse wake field calculations are usually performed for only a few higher modes $p > 0$. Therefore, the required memory and the calculation time are almost same order as 2-D simulations.

Finally, we mention the applicability of the 2.5-D S-TDBEM scheme based on the azimuthal Fourier expansion. Although we start here the discussion from the assumption of a bunch of linear path (14), the azimuthal expansion can be used for the curved path case as well if the self-field of a curved trajectory bunch can be azimuthally expanded. Only the requirements are: the problem is linear and the geometry is axially symmetric.

D. Moving Window Technique

In order to compute the short-range wake fields of a short bunch traversing long accelerator structures at low calculation costs, we can apply the integral equation formulation of moving window technique [11] into the full 3-D, A3D and 2.5-D S-TDBEM schemes presented above. The implementations of the moving window technique for their S-TDBEM

Authorized licensed use limited to: HOKKAIDO DAIGAKU KOHGAKUBU. Downloaded on September 7, 2009 at 03:22 from IEEE Xplore. Restrictions apply.

schemes are straightforward. Here we summarize some features of the moving window technique in the framework of TDBEM.

It can be understood immediately that implicit schemes (the matrix $[G_0]$ is non-diagonal) cannot be available for the moving window technique in principle because a part of the off-diagonal elements of the matrix $[G_0]$ is corresponding to the contribution of boundary values outside the moving window, and thus the lack of boundary value information at the tail of moving window arises. Therefore, we need to use explicit scheme (the matrix $[G_0]$ is diagonal) for the system matrix (13). The inversion of the matrix $[G_0]$ can be easily performed.

The technique presented in [11] brings us drastic savings of required memory in the above S-TDBEM schemes. Then, the calculation time in turn becomes the most significant problem in computational point of view because the number of the reduced coefficient matrices still depends linearly on the total length of an accelerator structure (in realistic accelerator problems the transverse dimension of a structure is usually much smaller than the longitudinal size). The number of the time steps increases linearly as well. Hence, the computational effort scales quadratically with the total length. This quadratic scaling law is a main drawback of the moving window technique of TDBEM compared to the moving window implementation in FIT scheme because the scaling is only linear in a FIT scheme with moving window technique. For this problem, a parallelization algorithm [11] has been proposed. This can be also applied to the full 3-D, A3D and 2.5-D S-TDBEM schemes.

This moving window technique is available even if a bunch has curved trajectories when the bunch has very high energy and always moves inside a moving window. This application example will be demonstrated in Section IV.

E. Self-Field Calculation for a Beam Moving With Curved Trajectory

The S-TDBEM formulation requires the calculation of the bunch self-fields on the boundary surface of a structure in (8). In this work, a free space field solver has been developed based on (4) and (5). In the following we briefly summarize an algorithm implemented in the free space field solver.

As mentioned in Section II, the self-field of a bunch of charged particles moving with general trajectories in free space can be calculated from the retarded potential formula of electric and magnetic fields (4) and (5). For a one-dimensional (line) bunch, the electric and magnetic self-fields in free space are represented as

$$\mathbf{E}_{self}(\mathbf{r},t) = -\frac{\mu_0}{4\pi}\frac{\partial}{\partial t}\int_{-\infty}^{\infty}\frac{\mathbf{J}(s',t')}{|\mathbf{r}-\mathbf{r}'|}ds' + \frac{1}{4\pi\varepsilon_0} \cdot \int_{-\infty}^{\infty}\left(\frac{\mathbf{r}-\mathbf{r}'}{|\mathbf{r}-\mathbf{r}'|^3}+\frac{\mathbf{r}-\mathbf{r}'}{|\mathbf{r}-\mathbf{r}'|^2}\frac{\partial}{c\partial t}\right)\rho(s',t')ds' \quad (21)$$

$$\mathbf{B}_{self}(\mathbf{r},t) = -\frac{\mu_0}{4\pi} \cdot \int_{-\infty}^{\infty}\left[\left(\frac{\mathbf{r}-\mathbf{r}'}{|\mathbf{r}-\mathbf{r}'|^3}+\frac{\mathbf{r}-\mathbf{r}'}{|\mathbf{r}-\mathbf{r}'|^2}\frac{\partial}{c\partial t}\right)\times\mathbf{J}(s',t')\right]ds' \quad (22)$$

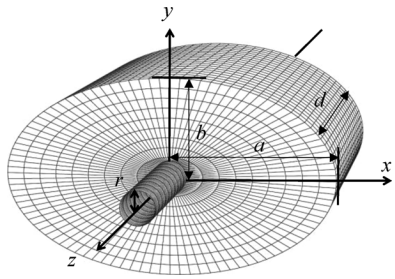

Fig. 4. Numerical model of elliptical pillbox cavity with small beam pipes.

with a given source distribution

$$\rho(s',t)=\lambda(s'(\mathbf{r}')-v't),\ \mathbf{J}(s',t)=\lambda(s'(\mathbf{r}')-v't)\,\mathbf{v}(t), \quad (23)$$

$s'=s'(\mathbf{r}')$, $\mathbf{r}'=\mathbf{r}'(s')$, $\mathbf{v}'=d\mathbf{r}'(t')/dt'$, $v'=|\mathbf{v}'|$ and the retarded time

$$t'=t-\frac{|\mathbf{r}-\mathbf{r}'(s')|}{c}. \quad (24)$$

For a finite length of bunch, the retarded fields (21), (22) can be computed by 1-D numerical integrations over non-vanishing retarded sources. More detailed discussions and treatment of other bunch shapes can be founded in [18].

IV. Numerical Examples

In this section, we demonstrate several numerical examples with the proposed schemes.

A. Elliptical Pillbox Cavity

In order to test the full 3-D S-TDBEM code, we simulate wake fields in an elliptical pillbox cavity of $a=5\,\mathrm{cm}$, $b=3\,\mathrm{cm}$, $d=10\,\mathrm{cm}$ which is connected to small beam pipe radius r as shown in Fig. 4. An analytical solution based on modal expansions is well-known for a closed elliptical cavity [19]. This analytical solution provides a good approximation in order to validate fully 3-D wake field calculations in the case of a Gaussian bunch with much longer RMS length σ than r.

Fig. 5 demonstrates the comparison of wake potentials calculated by the full 3-D S-TDBEM code and the analytical solution for the elliptical cavity. The implicit scheme has been used in this full 3-D calculation. An iterative matrix solver for $[G_0]$ in (13) is based on the conjugate gradient squared (CGS) method. In each time step of this simulation, the number of iteration operated in the CGS solver was less than 15. The total number of boundary elements is 7080 and the number of the coefficient matrix $[G_k]$ is 38. The used mesh size h is $\sigma/7.5$ in the z-direction, and then the calculation time is 33 minutes and the required memory is about 70 GB. The numerical result is converged to the analytical solution of the closed cavity as r is decreased. We can confirm the validity of the developed full 3-D S-TDBEM code.

Next, we test numerical convergence of the full 3D S-TDBEM scheme in the elliptical pillbox cavity model with beam pipe of $r=5\,\mathrm{mm}$. The convergence result of the proposed 3-D scheme for the elliptical pillbox cavity is shown

Authorized licensed use limited to: HOKKAIDO DAIGAKU KOHGAKUBU. Downloaded on September 7, 2009 at 03:22 from IEEE Xplore. Restrictions apply.

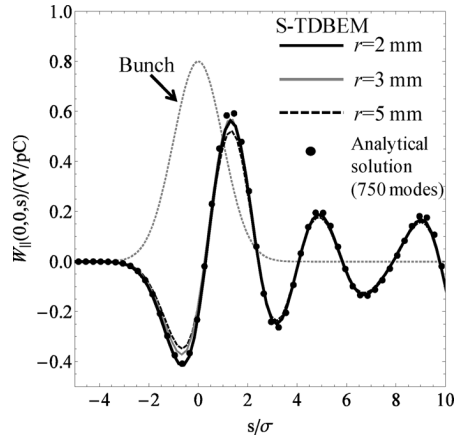

Fig. 5. Longitudinal wake potential of a Gaussian bunch ($\sigma = 2.5$ cm) traversing an elliptical pillbox cavity. The 3-D S-TDBEM calculations are done for different beam pipe radii. Three curves follow the analytical solution.

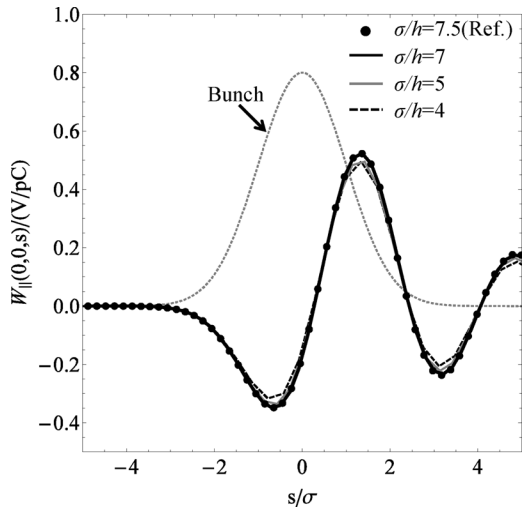

Fig. 6. Convergence of longitudinal wake potential of the elliptical pillbox cavity calculated with the full 3-D S-TDBEM code.

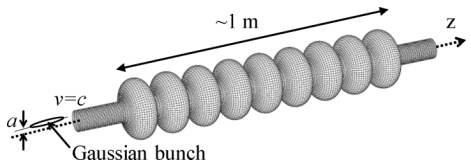

Fig. 7. Numerical model of TESLA 9cell cavity. A Gaussian bunch with an offset a to the z-axis is passing through the TESLA 9cell cavity.

in Fig. 6. We can find that the solution is almost converged for $\sigma/h = 7$.

B. TESLA 9cell Cavity

As an example of wake field analysis with the proposed 2.5-D S-TDBEM scheme, we demonstrate simulation results for short-range wake fields excited by an off-axis Gaussian bunch traversing inside the TESLA 9cell cavity [20] as shown in Fig. 7. In this simulation, we have used the 2.5-D S-TDBEM code combined with the moving window technique [11].

Fig. 8 demonstrates longitudinal dipole (azimuthal mode $p = 1$) wake potentials for RMS length $\sigma = 5$ mm and transverse

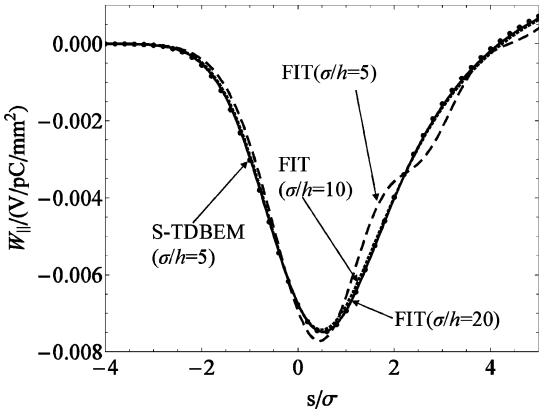

Fig. 8. Longitudinal dipole wake potential calculated with a simple 2.5-D FIT scheme with square mesh and 2.5-D S-TDBEM scheme for the TESLA 9cell cavity excited by a Gaussian bunch with $\sigma = 5$ mm and with an offset $a = 1$ mm to the axis.

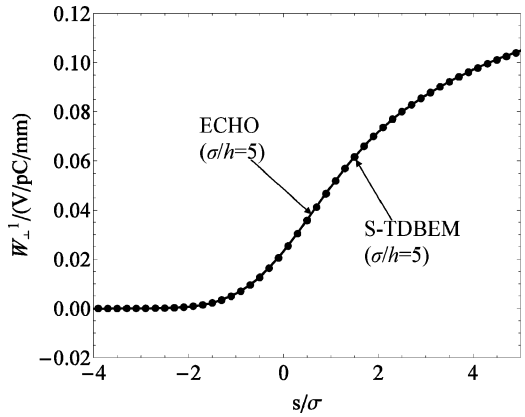

Fig. 9. Comparison of transverse dipole wake potentials calculated by different dispersion-free codes for the TESLA 9cell cavity excited by a Gaussian bunch with $\sigma = 2$ mm and with an offset ($a = 1$ mm) to the axis. The both calculations are done with a coarse mesh resolution ($\sigma/h = 5$).

offset $a = 1$ mm obtained with different numerical schemes. The FIT results are computed with the standard 2.5D scheme [16] based on azimuthal mode expansion with square mesh in cylindrical coordinates. This FIT code does not incorporate the moving window technique. Due to the dispersion error of the used FIT scheme, oscillation is observed in the coarse mesh result ($\sigma/h = 5$, where h is spatial mesh size) of wake potential calculated with the 2.5-D FIT scheme. In the 2.5-D S-TDBEM results, there is no oscillation even for the coarse mesh $\sigma/h = 5$ because of the grid dispersion-free property. The FIT result for $\sigma/h = 20$ converges to the S-TDBEM result.

Fig. 9 shows the comparison of transverse dipole wake potentials of a shorter Gaussian bunch with $\sigma = 2$ mm and transverse offset $a = 1$ mm calculated by the 2.5-D S-TDBEM code and the 2.5-D ECHO code [21]. The ECHO code incorporates the moving window technique and is based on a conformal FIT scheme without numerical grid dispersion in the longitudinal direction of beam motion. With the same mesh resolution $\sigma/h = 5$, we can find very good agreement between the S-TDBEM and the ECHO results. The S-TDBEM calculation is performed on a supercomputer, the HITACHI SR-11000. The calculation time is about 39 hours. The ECHO calculation

Authorized licensed use limited to: HOKKAIDO DAIGAKU KOHGAKUBU. Downloaded on September 7, 2009 at 03:22 from IEEE Xplore. Restrictions apply.

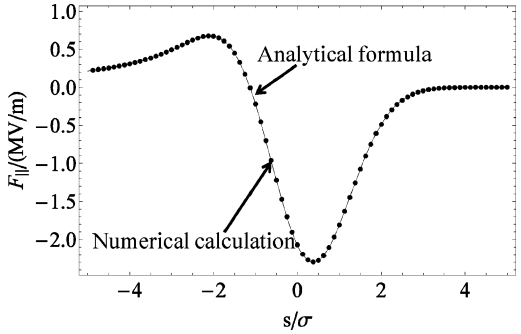

Fig. 10. Longitudinal component of the normalized Lorentz force generated by a Gaussian line bunch obtained by the numerical calculation based on (4), (5) and the analytical formula [22], [23]. The calculation parameters are same as [24]: $\sigma = 50\ \mu\mathrm{m}$, $q = 1\ \mathrm{nC}$, bending radius $R = 1.5$. The observation point is $s = \mathrm{ordinate}$, offsets $\Delta r = 0$, $\Delta z = 10\ \mu\mathrm{m}$.

is done on a standard PC with Intel(R) Core(TM) 2 CPU 1.66 GHz/1.67 GHz. The calculation time is about 4.5 minutes.

C. Wake Field of 1-D Gaussian Bunch Moving on Circular Orbit in Free Space

Here we show comparison of a numerical result based on (21), (22) with the well-known analytical result for wake field generated by a bunch moving on a circular orbit in free space [22], [23] as a preliminary validation test of the S-TDBEM code which solves wake fields excited by a bunch moving with curved trajectories in arbitrary 3-D vacuum chamber geometries. Fig. 10 demonstrates the longitudinal component of the normalized Lorentz force $\mathbf{F} = \mathbf{E} + \mathbf{v} \times \mathbf{B}$ generated by a Gaussian line bunch on a circular path with radius $R = 1.5\,\mathrm{m}$ in free space. We can see that the numerical result based on (21), (22) is agree with the analytical result.

D. Synchrotron Radiation Shielded by a Pipe-Like Vacuum Chamber With Circular Cross Section

Finally, we demonstrate a time domain simulation of wake fields on a bunch moving with a curved trajectory in a pipe-like vacuum chamber with circular cross section as in Fig. 11(c). This simulation is a typical example for which the existing numerical code cannot be applied.

For this simulation, we combined the explicit full 3-D S-TDBEM solver (including the moving window technique) with the free space field solver for the calculation of the self-field of curved trajectory described in Section III-E. Each solver is carefully verified as in the previous sections. The synchrotron radiations emitted from the bunch itself are simulated by the developed free space field solver. The shielding effects of coherent synchrotron radiation (CSR) by the vacuum chamber shown in Fig. 11(c) are included in the developed S-TDBEM solver. Additionally, we developed a field solver based on the well-known image charge method for parallel plate approximation of the vacuum chamber (similar to [24]) by modifying the developed free space field solver. The verification of this parallel plate solver was made by comparison with the results shown in [24].

The chamber geometry to be numerically modeled consists of the two parts: straight beam pipe section for upstream part and the remaining toroidal circular pipe section at downstream part. The bunch trajectory is given along the axis of the two pipe sections. For simplicity, the bunch charge distribution is assumed to be one-dimensional and fixed Gaussian along the given trajectory characterized by path length s.

The calculation parameters are: the radius of circular cross-section $r = 4\,\mathrm{cm}$, total charge $Q = 1\,\mathrm{nC}$, the Gaussian bunch parameter $\sigma = 1\,\mathrm{cm}$, the 1 GeV bunch energy, and the bending radius of the toroidal pipe section $R = 1.5\,\mathrm{m}$. The entrance of the toroidal chamber section is taken to be $s = 0$. The field calculation is performed with the initial position of the bunch center $s_c = -0.5572\,\mathrm{m}$, total time step $N_t = 1000$ and $c\Delta t = 1.0\,\mathrm{mm}$.

Fig. 12 shows longitudinal and transverse components of the normalized Lorentz forces $\mathbf{F} = \mathbf{E} + \mathbf{v} \times \mathbf{B}$ on the bunch trajectory at the final time step computed by (A) the full 3D S-TDBEM code with the moving window technique and (B) the image charge method based on the parallel plate approximation of the chamber [24], and (C) the free space model. For avoiding the singularity of 1-D line bunch, the observation points have an offset $d = 3\,\mathrm{mm}$ to the bunch trajectory. With the given model parameters, we can roughly estimate the overtaking length $L_o = (24\sigma R^2)^{1/3} = 0.814\,\mathrm{m}$, and the bunch center position for the field distribution at the final time step is about 0.44 m. Therefore, the fields shown in Fig. 12 still are in transient states. In both the circular pipe model and the parallel plate model (gap distance $g = 8\,\mathrm{cm}$), the shielding effects for the self-field are obviously observed due to the existence of chamber boundaries. We can understand that the differences of strength and phase of the fields occur due to difference of cross section geometries. Accordingly, it is found that appropriate modeling of vacuum chamber geometry is necessary to accurately take into account shielded effects of a curved trajectory beam in real chamber systems.

V. Conclusion

Three-dimensional wake field simulations are presented which are based on full 3-D, and 2.5-D S-TDBEM schemes. The developed full 3-D/2.5-D codes have been applied for the elliptical pillbox cavity and the TESLA 9cell cavity. The numerical results have been compared with the analytical solution and those of the latest FIT codes. Good agreements have been demonstrated in the numerical examples.

In addition to the above numerical simulation for validity check of the S-TDBEM codes, this paper presents transient analysis of coherent synchrotron radiation (CSR) shielded by the curved beam pipe chamber as the most promising application of the TDBEM in wake field analysis. The numerical results have been compared with the results by the parallel plate approximation based on the image charge method.

The next step in the S-TDBEM wake field analysis is to combine the developed full 3-D S-TDBEM scheme with a particle tracking code, and to apply it to self-consistent particle dynamics simulation with CSR field and space charge forces. This application will be presented in near future.

As another future work, there is resistive wall wake field calculations based on S-TDBEM.

Authorized licensed use limited to: HOKKAIDO DAIGAKU KOHGAKUBU. Downloaded on September 7, 2009 at 03:22 from IEEE Xplore. Restrictions apply.

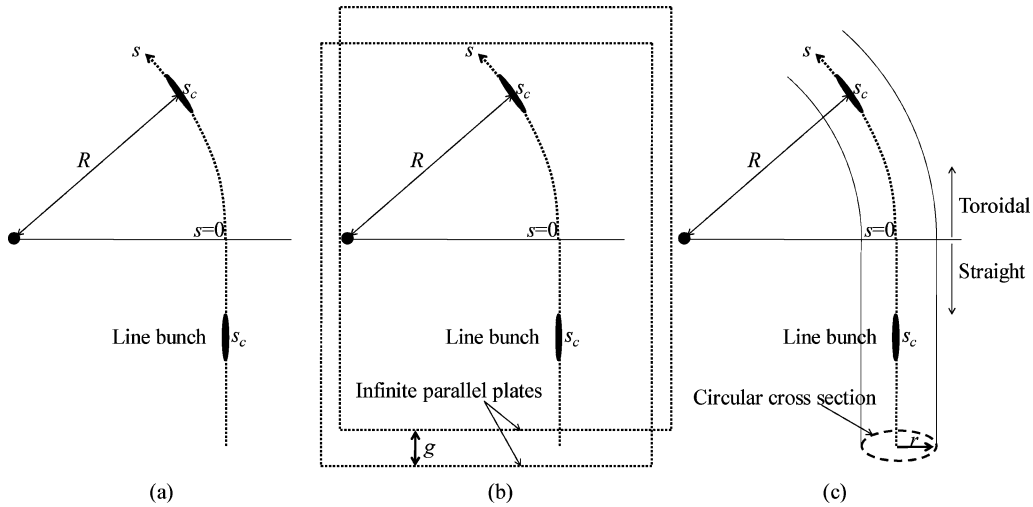

Fig. 11. Vacuum chamber geometries tested for transient analysis of wake fields generated by a Gaussian line bunch moving with curved trajectory. (a) Free space model, (b) infinite parallel plate model, (c) pipe-like vacuum chamber with circular cross section.

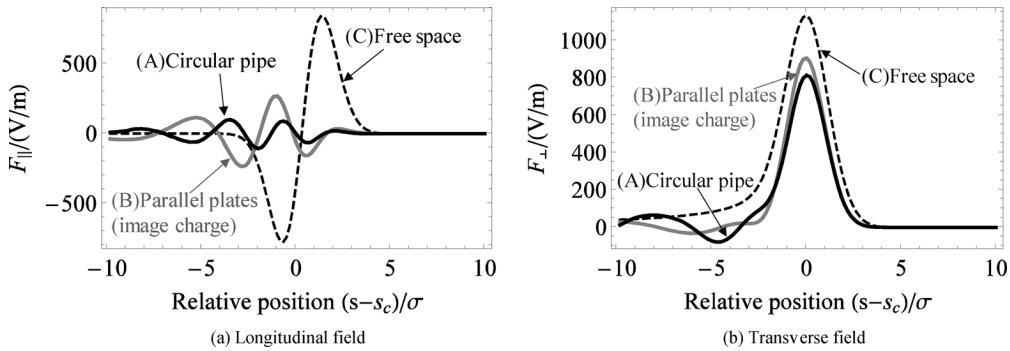

Fig. 12. Longitudinal and transverse field components of the normalized Lorentz forces excited by a Gaussian line bunch with a curved trajectory calculated by the two different vacuum chamber geometries. The calculation parameters are: the radius of circular cross-section $r = 4$ cm, total charge $Q = 1$ nC, the Gaussian bunch parameter $\sigma = 1$ cm, the 1 GeV bunch energy, and the bending radius of the toroidal pipe section $R = 1.5$ m. In the parallel plate model, the gap distance g between the two plates is 8 cm $= 2r$. The entrance of the toroidal chamber section is corresponding to $s = 0$ and the field calculation is done with the initial position of the bunch center $s_c = -0.5572$ m, total time step $N_t = 1000$ and $c\Delta t = 1.0$ mm. (A) Circular pipe (S-TDBEM), (B) parallel plate model (image charge), (C) free space.

REFERENCES

[1] B. W. Zotter and S. A. Kheifets, *Impedances and Wakes in High-Energy Particle Accelerators*. Singapore: World Scientific, 1998.

[2] T. Weiland, "Time domain electromagnetic field computation with finite difference methods," *Int. J. Numer. Model.: Electron. Networks*, vol. 9, p. 295, 1996.

[3] A. Candel *et al.*, "Parallel higher order finite element method for accurate field computations in wake field and PIC simulations," in *Proc. Int. Conf. Atomic Physics*, Chamonix, France, 2006.

[4] R. Hampel, I. Zagorodnov, and T. Weiland, "New discritization scheme for wake field computation in cylindrically symmetric structures," in *Proc. Euro. Particle Accelerator Conf.*, Lucerne, Switzerland, 2004, pp. 2559–2561.

[5] E. Gjonaj *et al.*, "Large scale parallel wake field computation for 3D-accelerator structures with the PBCI code," in *Proc. Int. Conf. Atomic Physics*, Chamonix, France, 2006, pp. 29–34.

[6] M. Kärkkäinen, E. Gjonaj, T. Lau, and T. Weiland, "Low-dispersion wake field calculation tools," in *Proc. Int. Conf. Atomic Physics*, Chamonix, France, 2006, pp. 35–40.

[7] R. Hampel, W. F. O. Muller, and T. Weiland, "ROCOCO-A zero dispersion algorithm for calculating wake potentials," in *Proc. Int. Conf. Atomic Physics*, Chamonix, France, 2006, pp. 144–147.

[8] H. Kawaguchi, "Stable time-domain boundary integral equation method for axisymmetric coupled charged-electromagnetic field problems," *IEEE Trans. Magn.*, vol. 38, pp. 749–752, 2002.

[9] H. Kawaguchi, "Time-domain analysis of electromagnetic wave fields by boundary integral equation method," *Eng. Anal. Boundary Elements*, vol. 27, pp. 291–304, 2003.

[10] K. Fujita, H. Kawaguchi, I. Zagorodnov, and T. Weiland, "Time domain wake field computation with boundary element method," *IEEE Trans. Nucl. Sci.*, vol. 53, no. 2, pp. 431–439, Apr. 2006.

[11] K. Fujita, H. Kawaguchi, R. Hampel, W. F. O. Müller, T. Weiland, and S. Tomioka, "Time domain boundary element analysis of wake fields in long accelerator structures," *IEEE Trans. Nucl. Sci.*, vol. 55, no. 5, pp. 2584–2591, Oct. 2008.

[12] K. Fujita, H. Kawaguchi, S. Nishiyama, S. Tomioka, T. Enoto, I. Zagorodnov, and T. Weiland, "Scattered-field time domain boundary element method and its application to transient electromagnetic field simulation in particle accelerator physics," *IEICE Trans. Electron.*, vol. E90-C, no. 2, pp. 265–274, 2007.

[13] J. D. Jackson, *Classical Electrodynamics*, 3rd ed. New York: Wiley, 1999.

[14] J. Jin, *The Finite Element Method in Electromagnetics*, 2nd ed. New York: Wiley, 2002.

[15] A. Taflove, *Computational Electrodynamics: The Finite Difference Time Domain Method*, 3rd ed. Norwood, MA: Artech House, 2005.

[16] T. Weiland, "Transverse beam cavity interaction–Part I: Short range forces," *Nucl. Instrum. Methods*, vol. 212, pp. 13–34, 1983.

[17] Y. Chin, ABCI User's Guide (Azimuthal Beam Cavity Interaction), 1988, CERN LEP-TH/88-3.

[18] M. Dohlus, Two Methods for the Calculation of CSR Fields, 2003, TESLA-FEL-2003-05.

Authorized licensed use limited to: HOKKAIDO DAIGAKU KOHGAKUBU. Downloaded on September 7, 2009 at 03:22 from IEEE Xplore. Restrictions apply.

[19] J. S. Yang and K. W. Chen, "A closed-form solution of wake-fields in an elliptical pill-box cavity by using an elliptical coordinate system," in *Proc. Amer. Institute of Physics Conf.*, 1989, vol. 193, pp. 417–432.
[20] TESLA Technical Design Rep. Hamburg, Germany, 2001, DESY 2001-011, II.
[21] I. Zagorodnov and T. Weiland, "TE/TM field solver for particle beam simulations without numerical Cherenkov radiation," *Phys. Rev. ST Accel. Beams*, vol. 8, p. 042001, 2005.
[22] Y. S. Dervenev, J. Rossbach, E. L. Saldin, and V. D. Shiltsev, Microbunch Radiative Tail-Head Interaction, 1995, TESLA-FEL-96-14.
[23] Y. S. Dervenev and V. D. Shiltsev, Transverse Effects of Microbunch Radaitive Interaction, 1996, FERMILAB-TM-1974, SLAC-PUB-7181.
[24] M. Dohlus and T. Limberg, "Emittance growth due to wake fields on curved bunch trajectories," *Nucl. Instrum. Methods Phys. Res. A*, vol. A393, pp. 494–499, 1997.

Authorized licensed use limited to: HOKKAIDO DAIGAKU KOHGAKUBU. Downloaded on September 7, 2009 at 03:22 from IEEE Xplore. Restrictions apply.